KOREA ADVANCED INSTITUTE OF SCIENCE AND TECHNOLOGY
DEPARTMENT OF MECHANICAL ENGINEERING
373-1 KUSONG-DONG, YUSONG-GU, TAEJON 305-701, KOREA

CHOONGSIK BAE Ph.D., DIC Professor
Tel : 82-42-869-3044 Fax : 82-42-869-5023/5044 E-mail : csbae@kaist.ac.kr

Dear Principal Editor,

I am pleased to submit a paper script, which could be a contribution to the Fuel in automotive applications.

Please find the manuscript of a paper submitted to International Journal of Thermal Science.

Title of the manuscript ;

Knock Characteristics in LPG-DME and Gasoline-DME Homogeneous Charge Compression Ignition Engines

Authors ;

Kitae Yeom and Choongsik Bae

Here is the affiliation of three researchers working in the same field.

1. Professor, Dr. Hua Zhao; Brunel University

Address : Brunel University, Uxbridge, Middlesex, UB8 3PH,, UK

e-mail address : hua.zhao@brunel.ac.uk

2. Professor, Dr. Ulrich Spicher; University of Karlsruhe

Address : University of Karlsruhe, Kaiserstr 12, D76131 Karlsruhe, Germany

e-mail address : ulrich.spicher@ifkm.uni-karlsruhe.de

3. Dr. James Eng; Staff Research Engineer of General Motors

Address: 30300 Mound Rd, Warren, MI, 48092, USA

e-mail address : james.eng@gm.com

Please do not hesitate to contact me if you have any request for the process of review.

Best wishes.

Yours sincerely,

Choongsik Bae, PhD, DIC

Professor, Mech. Eng., KAIST

373-1 Kusong, Yusong, Taejon 305-701, KOREA

csbae@kaist.ac.kr

Tel : 82-42-869-3044, Fax : 82-42-869-5023

Knock Characteristics in LPG-DME and Gasoline-DME Homogeneous Charge Compression Ignition Engines

Kitae Yeom, Choongsik Bae
Korea Advanced Institute of Science and Technology

Abstract

The knock characteristics in an engine were investigated under homogeneous charge compression ignition (HCCI) operation. The high load operation of HCCI engine is limited by knock and high combustion pressure. In order to avoid the engine damage, the engine must be operated under knock limit. Liquefied petroleum gas (LPG) and gasoline were used as fuels and injected at the intake port using port fuel injection equipment. Di-methyl ether (DME) was used as an ignition promoter and was injected directly into the cylinder during the intake stroke. A commercial variable valve timing device was used to control the volumetric efficiency and the amount of residual gas. Different intake valve timings and fuel injection amounts were tested to verify the knock characteristics of the HCCI engine.

The intake valve open timing was varied from -29 to 11 crank angle degree after top dead center. The valve open duration was fixed at 228 crank angle degree. The λ_{TOTAL} was varied from 2.91 to 2.12 while, λ_{DME} was fixed at 3.7. The ringing intensity (RI),

which indicates the energy of pressure wave, was used to define the intensity of knock according to the operating conditions. The RI of the LPG-DME HCCI engine was lower than that of the gasoline-DME HCCI engine through all the experimental conditions. The indicated mean effective pressure dropped when the RI was over 0.5 MW/m^2 and the maximum combustion pressure was over 6.5 MPa. There was no substantial relationship between RI and fuel type. The RI can be predicted by measuring and calculating the crank angle degree of 50% mass fraction burned. Carbon monoxide and hydrocarbon emissions were minimized at high ringing intensity conditions. The shortest burn duration under 0.5 MW/m^2 of RI was effective in achieving low hydrocarbon and carbon monoxide emissions.

Keywords : HCCI (homogeneous charge compression ignition), Knock, LPG (liquefied petroleum gas), Gasoline, DME (di-methyl ether)

Nomenclature

γ	specific heat ratio
λ	relative air/fuel ratio
θ	crank angle degree
ρ_a	inlet air density
A	air
F	fuel
$\dot{m}_a$	mass air flow rate

$\dot{m}_f$	mass fuel flow rate
N	number of cycles
P	cylinder combustion pressure
$(\frac{\partial p}{\partial t})_{\max}$	maximum pressure rise
R	universal gas constant
Q	heat release
T	temperature
V	cylinder volume
V_d	displacement volume

Abbreviations

AC	alternating current
ABDC	after bottom dead center
ATDC	after top dead center
BBDC	before bottom dead center
BTDC	before top dead center
CAD	crank angle degree
CI	compression ignition
CO	carbon monoxide
CO_2	carbon dioxide
DI	direct injection

DOHC	double over head camshaft
DME	di-methyl ether
ECU	engine control unit
HC	hydrocarbon
HCCI	homogeneous charge compression ignition
HTR	high temperature reaction
IMEP	indicated mean effective pressure
IMPG	integral of modulus of pressure gradient
IMPO	integral of modulus of pressure oscillation
IVO	intake valve open
LHV	low heating value
LPG	liquefied petroleum gas
LTR	low temperature reaction
MAPO	maximum amplitude of pressure oscillation
MFB	mass fraction burned
NOx	nitric oxide
RI	Ringing intensity
SI	spark ignition

TDC	top dead center
VVT	variable valve timing

Subscripts

a	air
d	displacement
DME	di-methyl ether
gasoline	gasoline
LPG	liquefied petroleum gas
max	maximum
total	total
v	volumetric

1. Introduction

The homogeneous charge compression ignition (HCCI) engine is regarded one of the futural engine technologies due to its superior nitric oxide (NOx) emissions and fuel economy characteristics [1]. The nature of the HCCI engine is a combination of spark ignition (SI) and compression ignition (CI) engines in its mixture preparation and

ignition process, respectively [1]. The HCCI engine breathes premixed charge and ignites the premixed charge by heat and pressure due to compression. The start of HCCI combustion originates from a chemical reaction which is initiated by compression heat and pressure [1]. This chemical reaction occurs at every single point of the combustion chamber simultaneously. Due to simultaneous combustion, the combustion duration of HCCI is very short [2]. A higher compression ratio or larger amount of residual gas is needed to ignite the charge with high octane number fuels, such as gasoline and liquefied petroleum gas (LPG) [3]. However, these two ignition promotion methods also accelerate the speed of combustion. Fast and early combustion leads to a higher combustion pressure and a higher rate of pressure rise [1].

The combustion of HCCI is very similar to the knock phenomenon in SI engine operation due to its simultaneous self-ignition [4]. SI knock is the autoignition of the end gas ahead of the normal flame front [5,6]. In the case of SI engines, the spark timing for the best torque is limited by knock [6]. Similarly, the HCCI engine operating range is limited by high combustion pressure, high rate of pressure rise, and heavy knock [7,8]. The knock intensity and the effectiveness of the combustion phase method must be quantified to verify and expand the operating range.

An SI knock analysis based on cylinder pressure can be performed quantitatively, using the methods based on the items below [4] :

1. the evaluation of a single pressure value.

2. pressure derivatives.

3. frequency domain manipulations.

4. heat release analysis.

The knock intensity could be represented by the peak combustion pressure. However, the peak combustion pressure can be changed according to the operating conditions of test engine [4]. To overcome this defect, the rate of pressure rise was used. In this case, the minimum value of the third derivative of pressure was used as an indicator of knock intensity for minimum disturbance [9]. A method using the window energy at the frequency domain of knock has also been reported [10]. Three indices of knock intensity on the basis of a number of band pass-filtered cylinder pressure signals were used~~,~~ such as integral of modulus of pressure gradient (IMPG), integral of modulus of pressure oscillation (IMPO) and maximum amplitude of pressure oscillation (MAPO) [11-13].

~~follows [11-13] :~~

~~Integral of modulus of pressure gradient (IMPG)~~

~~IMPG= $\frac{1}{N}\sum_{1}^{N}\sum|\Delta p|$ (1)~~

~~Integral of modulus of pressure oscillation (IMPO)~~

~~IMPO= $\frac{1}{N}\sum_{1}^{N}\sum|p|$ (2)~~

~~Maximum amplitude of pressure oscillation (MAPO)~~

~~MAPO= $\frac{1}{N}\sum_{1}^{N}|p|_{max}$ (3)~~

A new method which can represent the knock intensity of HCCI combustion is needed due to its different combustion nature, and, therefore, the ringing intensity (RI) was introduced [14]. The RI indicates the wave energy of pressure oscillation due to knock [14]. The RI is shown as below :

$$RI=\frac{1}{2\cdot\gamma}\cdot\frac{\sqrt{\gamma RT}}{P}\cdot\frac{1}{N}\cdot\sum_{1}^{N}[0.05\cdot(\frac{\partial p}{\partial t})_{max}]^2 \quad (4)$$

where

γ	specific heat ratio
P	cylinder combustion pressure
R	universal gas constant
T	temperature
N	number of cycles
$(\frac{\partial p}{\partial t})_{max}$	maximum pressure rise

The use of RI for HCCI knock intensity has been reported [15,16].

In this paper, the knock intensity of LPG and gasoline HCCI using variable valve timing (VVT) and di-methyl ether (DME) direct injection in an engine was examined. The limits in operating range of test engine are defined by knock analysis and expanded by combustion phase control, using VVT. The knock intensity method was used to define the operating range. The effects of LPG, residual gas, and volumetric efficiency were also investigated to find the ways of widening the operating range.

2. Experimental apparatus and methods

2.1 Experimental apparatus

The specifications of the engine are given in Table 1. The base engine is a 4-cylinder spark ignition engine and has a double overhead camshaft (DOHC) equipped with VVT. A cylinder was modified for HCCI combustion with a DME direct injection system on the cylinder head. An engine control unit (ECU) (Motec Co., M4) was employed to precisely control DME quantity and injection timing. A second ECU (ETAS Co.) was used to control the quantity and timing of port fuel injection and intake valve timing.

Figure 1 shows a schematic diagram of the experimental setup. The engine speed and load were controlled with an alternating current (AC) dynamometer. A liquid phase

injection system was used for LPG injection into the intake manifold. This system can improve the volumetric efficiency via liquid phase injection and lower the intake air temperature owing to the heat absorption during LPG vaporization at the intake port. Additionally, reduced engine emissions can be achieved with precise mixture control, as in gasoline SI engines. A slit injector (Denso Co.) was used to inject DME directly into the cylinder at a constant supply pressure of 5 MPa, using pressurized nitrogen gas. The DME injector was located at the spark plug hole of the research engine. A lubricity enhancer (Infineum, R655) of 500 ppm was added to the DME to avoid damage to the fuel injection system. The in-cylinder pressure was measured using a piezoelectric pressure transducer (Kistler, 6052b). Short time drift of cylinder pressure sensor due to thermal shock is under ± 0.05 MPa. The intake and exhaust manifold pressures were measured by two piezo-resistive pressure transducers (Kistler, 4045A5). The intake and exhaust temperatures were measured with two K-type thermocouples, which were fitted on the intake and exhaust manifolds. A wide-band lambda meter (ETAS, LA4) was installed for the measurement of the relative air/fuel ratio. Exhaust gases were analyzed with a gas analyzer (Horiba, Mexa 1500d) to measure the HC, NOx, CO, and CO_2 emissions. Two data acquisition system (IOtech, Wavebook 512H) were employed to acquire all engine combustion and exhaust gas

data. A/D resolution, speed and accuracy are 12 bit, 1 MHz and ± 0.025% of full scale, respectively. The combustion, intake and exhaust pressure data were acquired with 34 kHz sampling rate. The others data including mass air flow rate and exhaust gases were acquired with 1 kHz sampling rate.

The VVT system can freely vary the open and close timing of intake valve. The intake valve open (IVO) timing was varied over a range of 29 crank angle degrees (CAD) before top dead center (BTDC) to 11 CAD after top dead center (ATDC), while the valve duration was fixed at 228 CAD. Generally, volumetric efficiency and residual gas increase as IVO timing is advanced at low engine speeds. The start of HCCI combustion is affected by surrounding conditions such as pressure, fuel distribution and temperature of mixture during compression stroke [1]. The temperature and pressure of charge are increased and reach earlier to the auto-ignition point, when the volumetric efficiency and residual gas fraction are higher, due to the combustion enhancement.

2.2 Experimental conditions

Table 2 shows the main experimental conditions used in this study. Relative air/fuel ratio, λ, is defined as the ratio $(A / F)_{actual} / (A / F)_{stoichiometric}$ [17]. The air fuel ratio, A /

F, is defined as the ratio $\dot{m}_a / \dot{m}_f$ [17]. In order to define the λ of each fuel, the total mass of fresh air and the injection quantity of each fuel were used.

λ_{TOTAL} is defined as shown in equation (5), which was derived from chemical oxidation formula of different λ_{TOTAL} condition.

$$\lambda_{TOTAL} = \frac{\lambda_{LPG}\lambda_{DME}}{\lambda_{LPG} + \lambda_{DME}} \qquad (5)$$

λ_{DME} was fixed at 3.7 and λ_{TOTAL} was varied from 2.12 to 2.91. The engine was run at 1000 rpm for various intake valve timings and air excess ratios. The proportions of propane and butane in the LPG used in this study were 60% and 40%, respectively. Figure 2 shows the intake valve timing and the DME injection timing. The intake valve open (IVO) timing was varied from -29 CAD ATDC to 11 CAD ATDC. The volumetric efficiency was 80% at an IVO timing of -29 CAD ATDC and 66.2% at an IVO timing of 11 CAD. The volumetric efficiency was calculated using equation (6) [17].

$$\eta_v = \frac{\dot{m}_a}{\rho_a V_d} \qquad (6)$$

where

$\dot{m}_a$ mass air flow rate

ρ_a inlet air density

V_d displacement volume

The mass flow rate of intake charge was measured using laminar flow meter (Meriam Co., 50MC2-2S). The DME injection timing was fixed at 110 CAD ATDC for the formation of a homogeneous mixture. Gasoline and LPG were injected into the intake manifold at 470 CAD ATDC.

2.3 In-cylinder pressure measurements and analysis

The piezoelectric pressure transducer for in-cylinder pressure measurement was flash-mounted inside the cylinder head to reduce pipe oscillation effects [18].

In order to analyze the pressure data precisely, a high-precision rotary encoder (2048 pulse/rev) was used for engine control and data acquisition. Typical pressure oscillation frequency of knock is approximately 5 kHz. The pressure data were acquired at every rotary encoder pulse, which is approximately 34 kHz at 1000 rpm of engine speed.

~~The present study focuses on the knock probability. In order to identify the knock, the criterion of pressure oscillation due to knock is defined as a pressure rise over 0.05 MPa during the expansion stroke [19]. The knock probability was calculated using equation (7).~~

$$\text{Knock probability (\%)} = \frac{number\ of\ cycles\ with\ knock}{100\ cycles} \times 100 \qquad (7)$$

The indicated mean effective pressure (IMEP) and heat release rate were calculated from the cylinder pressure values [17] using equation (8):

$$\frac{dQ}{d\theta} = \frac{\gamma}{\gamma - 1} P \frac{dV}{d\theta} + \frac{1}{\gamma - 1} V \frac{dP}{d\theta} + \Delta Q_{heattransfer} \qquad (8)$$

where

θ crank angle degree

γ specific heat ratio

P cylinder combustion pressure

Q heat release

V cylinder volume

The difference in lower heating values (LHV) of LPG and gasoline used in this study was less than 0.3%.

3. Experimental results

3.1 Ringing intensity analysis

Figure 3 shows the ringing intensity (RI) in HCCI combustion with gasoline and LPG, respectively, with respect to λ_{TOTAL} and intake valve open timing at 1000 rpm. The horizontal axis represents the intake valve open timing, and the vertical axis represents λ_{TOTAL}. The allowable operating range based on audible knock sounds is regarded as under 5 MW/m^2 of RI, which limit the high load operating range [15,16]. In the case of

gasoline-DME HCCI, the RI was over 5 MW/m^2 when λ_{TOTAL} was lower than 2.3, and the IVO timing was more advanced than -10 crank angle degrees. More than 50% of the fresh charge was burned, and the combustion pressure was rising before TDC at an early IVO timing. The RI increased as the IVO timing was advanced. This is attributed to increased volumetric efficiency and residual gas which promote combustion. Figure 4 shows the volumetric efficiency of test conditions. The volumetric efficiency was 80%, 79.5%, and 77.2% at the IVO timing of -29, -19, and -9 CAD ATDC, respectively. Furthermore, the volumetric efficiency dropped rapidly at 1 CAD ATDC and 11 CAD ATDC, with values of 70.8% and 66.2%, respectively.

The fresh charge temperature reached 800 ~ 1000K easily at the compression stroke due to the increased volumetric efficiency. The residual gas increased as the valve overlap period was increased [20]. The valve overlap period is the duration while the intake valve and the exhaust valve are open simultaneously. The exhaust gas is trapped by the pressure difference between the intake port and the exhaust port. The heat transfer from hot residual gas to the fresh charge increased, which promotes ignition [21]. The charge temperature reaches low temperature oxidation temperature, which is 600 ~ 900 K [1], more rapidly when the residual gas is more trapped in combustion chamber. In the case of LPG-DME, the RI did not exceed 5 MW/m^2 at any operating

condition. The reasons for the lower RI value of LPG-DME HCCI, compared to gasoline-DME HCCI, are the lower ~~cetane number~~self-ignitability of injected fuel and the ~~lower~~ larger latent heat of vaporization of total injected fuel. HCCI engine combustion is influenced by the chemical formation, temperature, and pressure of the air/fuel mixture [1]. The octane number of LPG used in this study is higher than gasoline [22]. Due to the low octane number, the gasoline-DME mixture has better ignitability than the LPG-DME mixture. The self-ignitability~~cetane number~~ and the latent heat of vaporization of LPG were the major reasons of late LPG-DME HCCI combustion. The self-ignitability~~cetane number~~ of total injected fuel decreased as λ_{TOTAL} decreased, due to lower λ_{LPG} and fixed λ_{DME}. The decrease in self-ignitability~~cetane number~~ of total fuel is one cause of late combustion [1]. Another cause is a lower intake temperature due to the latent heat of vaporization of LPG. The latent heat of vaporization of LPG used in this study is 370 kJ/kg, and that of gasoline is 306 kJ/kg. Due to the latent heat of vaporization, the temperature of the LPG/air mixture before the start of combustion was lower than that of the gasoline/air mixture by 2 K. In the case of the LPG-DME HCCI engine, the temperature of the air/fuel mixture is inversely proportional to the injection quantity of LPG. The octane number and temperature difference account for the difference in the start of combustion.

3.2 Combustion characteristics and knock probability

Figure 5 shows the effect of knock resulting from early combustion on the IMEP. This figure shows that λ_{TOTAL} is the major parameter of the IMEP in the case of gasoline-DME HCCI. There is an optimum amount of injected gasoline for attaining an optimal IMEP, corresponding to an approximate λ_{TOTAL} value of 2.4. When λ_{TOTAL} is lower than 2.4, the RI increases as IMEP drops rapidly. However, in the case of LPG-DME HCCI, the critical IMEP decrease was not observed. Higher volumetric efficiency and residual gas lead to early combustion, as explained. The RI, considered together with the IMEP, was more useful for the analysis of engine knock characteristics compared to the audible knock sounds. According to Figures 3 and 4, it was found that the IMEP was significantly affected by the RI value. The IMEP of the gasoline-DME and LPG-DME HCCI engines were decreased when the RI value was over 0.5 MW/m^2. This fact indicates that the high engine load should be limited to a certain range where the RI value is less than 0.5 MW/m^2.

Figure 6 shows the maximum combustion pressure (P_{max}) to identify the relationship between the RI and P_{max}. According to Figures 3 and 5, higher than 0.5 MW/m^2 of RI and lower than 0.27 MPa of IMEP show the operating conditions for which P_{max} was

over 6.6 MPa. This fact shows that most RI values higher than 0.5 MW/m^2 result from an over-pressure rise higher than 6.6 MPa due to early combustion.

The knock probability of LPG-DME and gasoline-DME HCCI engines, with respect to the RI, is shown in Figure 7. The knock probability of the HCCI engine is approximately 100% when the RI is over 0.5 MW/m^2. The knock probability of gasoline-DME and LPG-DME HCCI engines, with respect to the P_{max}, is shown in Figure 8. For every 25 engine operating conditions which were tested in this study, the relationship of the knock probability and the P_{max} of the gasoline-DME HCCI engine can be fit by the linear equation (9).

$$y = 47.2x - 215.15 \qquad (9)$$

The relationship of the knock probability and the P_{max} of the LPG-DME HCCI engine can be also fit by the linear equation (10).

$$y = 53.2x - 260.20 \qquad (10)$$

These two equations show the relationship between cylinder pressure and knock probability. The knock tendency of the LPG-DME HCCI engine was lower than that of the gasoline-DME HCCI engine. In the case of gasoline-DME HCCI, knock was occurring when the P_{max} was over 4.5 MPa. However, in the case of LPG-DME HCCI,

it was occurring when the P_{max} was over 4.9 MPa. However, the P_{max} of gasoline-DME and LPG-DME HCCI engines which lead to the knock probability of 100% were the same, approximately at 6.7 MPa. The knock probability can, therefore, be estimated by monitoring the combustion pressure.

3.3 Ringing intensity estimation

The RI with respect to CAD at 50% mass fraction burned (CA 50) of gasoline-DME and LPG-DME HCCI engines, is shown in Figure 9. The RI was increased as the CAD at CA 50 was advanced. The increase in the rate of the RI was reduced as λ_{TOTAL} increased. This is attributed to the reduction in the supplied LHV of the fuel. The RI that gradually increased from 0 MW/m^2 when the CA 50 was more advanced than that at 361 CAD. This graph shows that the combustion timing is another major factor of increased RI. The combustion phase control is needed to retard the CA 50 and to reduce the RI at high RI operating conditions. This trend shows that the fuel type had no effect on the RI and CAD at CA 50. The RI according to CAD at CA 50 could be fit well with a polynomial formulation, with a correlation coefficient R^2 over 0.95. Thus, the RI can be estimated by the CAD at CA 50 or the P_{max}.

3.4 Incomplete combustion and exhaust emissions

Figure 10 shows the ratio of carbon monoxide (CO) over carbon dioxide (CO_2) and hydrocarbon (HC) over all carbon contained in the exhaust emissions (CO, CO_2, and HC) with respect to RI of the gasoline-DME and LPG-DME HCCI engines at 1000 rpm. The mass fraction burned from 20% to 90%, with respect to RI, is shown in Figure 11.

The CO emissions of the HCCI engine are greater than those of SI or CI engines. This high CO emission is due to a lack of oxidation which has very close relationship with combustion temperature during the expansion stroke. Consequently, CO emission is regarded as the index of incomplete combustion for HCCI engines [1,2]. The CO oxidation is influenced by the in-cylinder temperature [23,24]. The higher peak combustion pressure led the higher combustion temperature. The CO/CO_2 ratio decreased as the RI increased. However, the CO/CO_2 ratio was approximately 0.17 at an RI of 0 MW/m^2. These facts show that the emission of CO was minimized due to maximized CO oxidation during the expansion stroke at an RI less than 0.5 MW/m^2 with high combustion temperature over 1500K [24].

Another problem of HCCI emission is the HC emissions [1]. The main source of HC emission is the captured fuel in the crevice volume of the combustion chamber. To

normalize the λ_{TOTAL} effect, the HC emission was divided by the exhaust emission, which contains carbon (CO, CO_2, HC), using equation (11) [2].

$$\text{Percentage of unburned fuel flow} = \frac{HC}{HC + CO + CO_2} \quad (11)$$

where

HC HC emission

CO CO emission

CO_2 CO_2 emission

The HC emission ratio decreased as the RI increased, and it was approximately 35 ~ 39%. However, the percentage of unburned fuel flow was almost 47% at low RI conditions. It attributed to the high quenching effects due to low combustion temperature. The CO/CO_2 ratio and HC emissions trends can be explained by the burn duration. Figure 11 shows the burn duration of the gasoline-DME and LPG-DME HCCI engines with respect to the RI. The RI is the index of knock intensity. However, the burn duration does not increase according to the RI. The burn duration was approximately 2 CAD at higher RI values. The reduced HC and CO emissions were the results of the high combustion temperature with short and vigorous combustion.

The most effective way to reduce HC and CO emissions in the HCCI engine is to achieve the shortest burn duration with low RI, which promotes the oxidation during the expansion stroke due to a higher combustion temperature.

4. Conclusions

The effects of ringing intensity (RI), combustion, and normalized exhaust emissions characteristics in LPG-DME and gasoline-DME HCCI engines, controlled by a variable valve timing (VVT), were investigated. Analysis of RI was performed in order to verify the HCCI combustion characteristics. The following conclusions were drawn from the experimental results.

1. The LPG-DME HCCI had wider operating range than gasoline-DME HCCI from an IMEP point of view. The LPG is more suitable for high load operation of HCCI than gasoline due to its high latent heat of vaporization and octane number.

2. The relationship between the IMEP and the RI showed that the IMEP of the gasoline-DME and LPG-DME HCCI engines decreased when the RI was over 0.5 MW/m^2. According to the IMEP decrease at relative air/fuel ratio of total injected fuel (λ_{TOTAL}) was lower than 2.4, the high load operating range of the test engine was

limited to under 0.5 MW/m^2. The reasons for the lower RI value of LPG-DME, compared to gasoline-DME HCCI, are the lower self-ignitability~~cetane number~~ of the total injected fuel and the latent heat of vaporization of injected LPG.

3. The RI increased as the intake valve open (IVO) timing advanced. This is attributed to higher volumetric efficiency and residual gas, which promotes combustion. More than 50% of the fresh charge was burned, and the combustion pressure was increasing before TDC at the early IVO timing due to higher volumetric efficiency and residual gas.

4. λ_{TOTAL} is the major parameter of IMEP. There is an optimum amount of injected gasoline for attaining optimal IMEP, corresponding to an approximate λ_{TOTAL} value of 2.4. When λ_{TOTAL} was lower than 2.4, the RI increased and IMEP dropped rapidly. However, in the case of LPG-DME HCCI, the IMEP dropped at a λ_{TOTAL} lower than 2.3, and the IVO timing advanced more than -10 CAD.

5. Higher RI and lower IMEP produced the operating conditions under which the P_{max} was over 6.5 MPa. Thus, most of the values of RI higher than 0.5 MW/m^2 resulted from a pressure rise greater than 6.5 MPa due to early combustion.

6. The RI can be estimated by the crank angle degree (CAD) at 50% mass fraction burned (CA 50) or the P_{max}. The RI increased as the CAD at CA 50 was advanced. The fuel type did not affect the RI and CAD at CA 50. The RI according to CAD at CA 50 could be fit well with a polynomial formula, and the R^2 of the fit was over 0.95.

7. The CO/CO_2 ratio decreased as the RI increased. However, the CO/CO_2 ratio was approximately 0.17 at an RI of 0 MW/m^2. These facts show that the emission of CO was minimized due to a maximized CO oxidation reaction during the expansion stroke at an RI of less than 0.5 MW/m^2. The HC emission ratio decreased as the RI increased. However, the burn duration did not increase according to the RI. The burn duration was approximately 2 CAD at higher RI values. The effective way to reduce the HC and CO emissions in a HCCI engine is the shortest burn duration with low RI which promotes the oxidation reaction during the expansion stroke due to a higher combustion temperature.

Acknowledgements

The authors would like to appreciate the Combustion Engineering Research Center (CERC) of the Korea Advanced Institute of Science and Technology (KAIST) for the financial support.

References

[1] Zhao F, Asmus T, Assanis D, Dec J, Eng J, Najt P. Homogeneous Charge Compression Ignition (HCCI) Engines : Key Research and Development Issues. SAE; 2003.

[2] Kaiser E, Yang J, Culp T, Xu N, Maricq M. Homogeneous Charge Compression Ignition Engine-Out Emissions-Does Flame Propagation Occur in Homogeneous Charge Compression Ignition?. Int J Engine Res 2002;3/4:185-96.

[3] Yap D, Karlovsky J, Megaritis A, Wyszynski M, Xu H. An Investigation into Propane Homogeneous Charge Compression Ignition Engine Operation with Residual Gas Trapping. Fuel 2005;84/18:2372-79.

[4] Millo F, Ferraro V. Knock in S. I. Engines : A Comparison between Different Techniques for Detection and Control. SAE transaction 1998;107/4:1090-111,982477.

[5] Abu-Qudais M. Exhaust Gas Temperature for Knock Detection and Control in Spark Ignition Engine. Energy Convers Manage 1996;37/9:1383-92.

[6] Seref Soylu. Prediction of knock limited operating conditions of a natural gas engine. Energy Convers Manage 2005;46/1:121-38.

[7] Griffiths J, MacNamara J, Sheppard C, Turton D, Whitaker B. The Relationship of Knock during Controlled Autoignition to Temperature Inhomogeneities and Fuel Reactivity. Fuel 2002;81/17:2219-25.

[8] Yeom K, Jang J, Bae C. Gasoline Homogeneous Charge Compression Ignition Engine with DME as an Ignition Promoter. Proc. 6th International Conference on GDI Engines 'Direkteinspritzung im Ottomotor / Gasoline Direct Injection Engines', expert verlag Jun 2005:229-39.

[9] Checkle M, Dale J. Computerized Knock Detection from Engine Pressure Records. SAE Technical Paper, No. 860028, 1986.

[10] Brunt M, Pond C, Biundo J. Gasoline Engine Knock Analysis using Cylinder Pressure Data. SAE transaction 1998;106/3:1399-412,980896.
[11] Brecq G, Ramesh A, Tazerout M. A New Indicator for Knock Detection in Gas SI Engines. Int J Thermal Sci 2003;42/5:523-32.
[12] Ramesh A, Brecq G, Tazerout M, Le Corre O. Knock Rating of Gaseous Fuels in a Single Cylinder Spark Ignition Engine. Fuel 2004;83/3:327-36.
[13] Hudson C, Gao X, Stone R. Knock Measurement for Fuel Evaluation in Spark Ignition Engines. Fuel 2001;80/3:395-407.
[14] Eng J. Characterization of Pressure Waves in HCCI Combustion. SAE Technical Paper, No. 2002-01-2859, 2002.
[15] Sjoberg M, Dec J. Effects of Engine Speed, Fueling Rate, and Combustion Phasing on the Thermal Stratification Required to Limit HCCI Knock Intensity. SAE transaction 2005;114/3:1472-86,2005-01-2125.
[16] Helmantel A, Denbratt I. HCCI Operation of a Passenger Car DI Diesel Engine with an Adjustable Valve Train. SAE Technical Paper, No. 2006-01-0029, 2006.
[17] Heywood J. Internal Combustion Engine Fundamentals. New York: McGraw Hill; 1988.
[18] Bertola A, Stadler J, Walter T, Wolfer P, Gossweiler C, Rothe M. Pressure indication during knocking conditions. 7th Internal Symposium on Internal Combustion Diagnostics, May 2006, Kurhaus Baden-Baden, Germany:7-21.
[19] Oakley A, Zhao H, Ladommatos N, Ma T. Dilution Effects on the Controlled Auto-Ignition (CAI) Combustion of Hydrocarbon and Alcohol Fuels. SAE transaction 2001;110/4:2086-99,2001-01-3606.
[20] Cavina N, Ponti F, Siviero C, Suglia R. Residual Gas Fraction Estimation for Model-Based Variable Valve Timing and Spark Advance Control. ASME Int Comb Engine Division 2004; ICEF2004-0956:457-66.
[21] Caton PA, Simon AJ, Gerdes JC, Edwards CF. Residual-effected Homogeneous Charge Compression Ignition at a Low Compression Ratio using Exhaust Reinduction. Int J Engine Res 2003;4/3:163-78.
[22] Yeom K, Jang J, Bae C. Homogeneous Charge Compression Ignition of LPG and Gasoline using Variable Valve Timing in an Engine. Fuel 2007;86/4:494-503.
[23] Bhave A, Kraft M, Montorsi L, Mauss F. Sources of CO emissions in an HCCI Engine: A Numerical Analysis. Combust. Flame 2006;144:634-37.
[24] Sjoberg M, Dec J. An Investigation into Lowest Acceptable Combustion Temperatures for Hydrocarbon Fuels in HCCI Engines. Proc. Combus. Inst. 2005;30:2719-26.

List of Figures

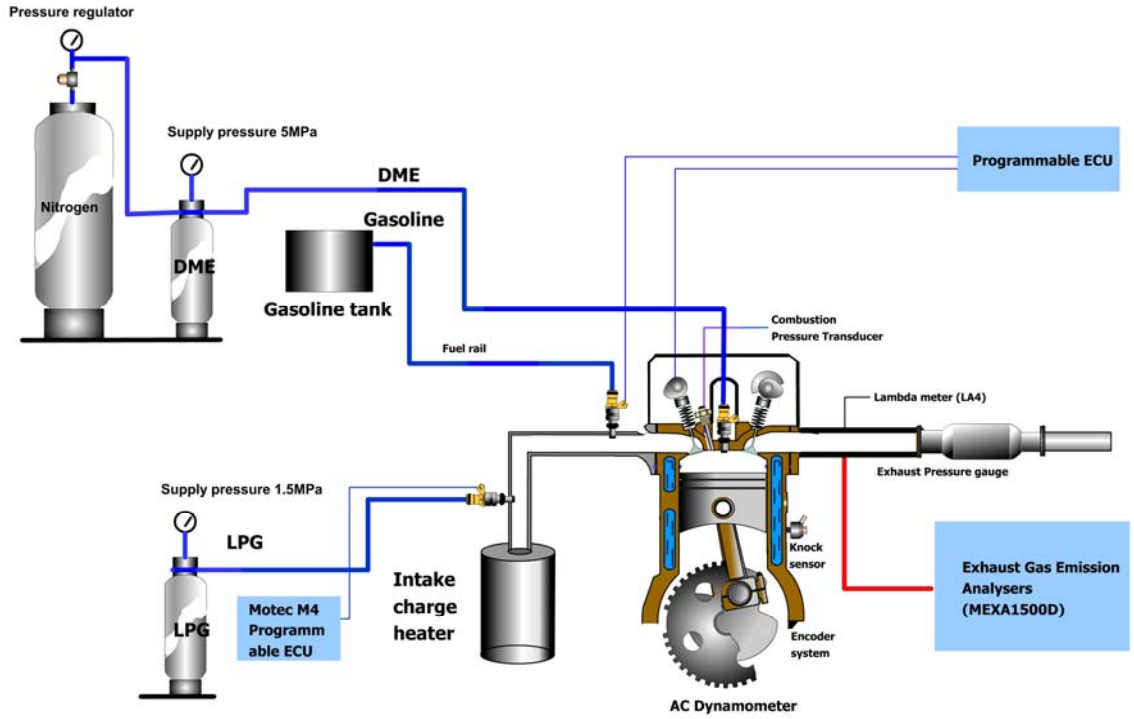

Figure 1 Schematic diagram of experimental apparatus

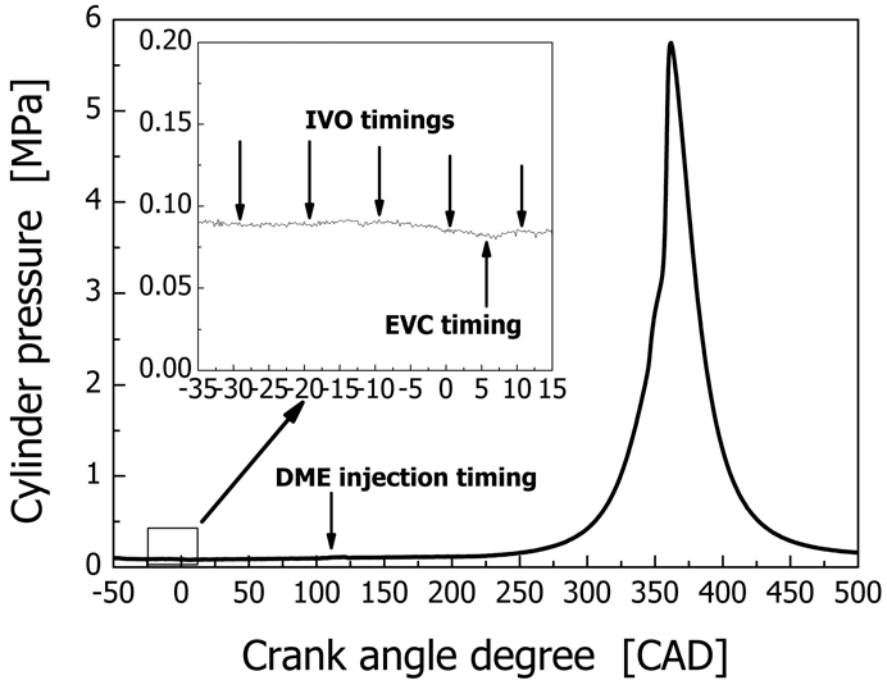

Figure 2 Intake valve open and DME injection timing

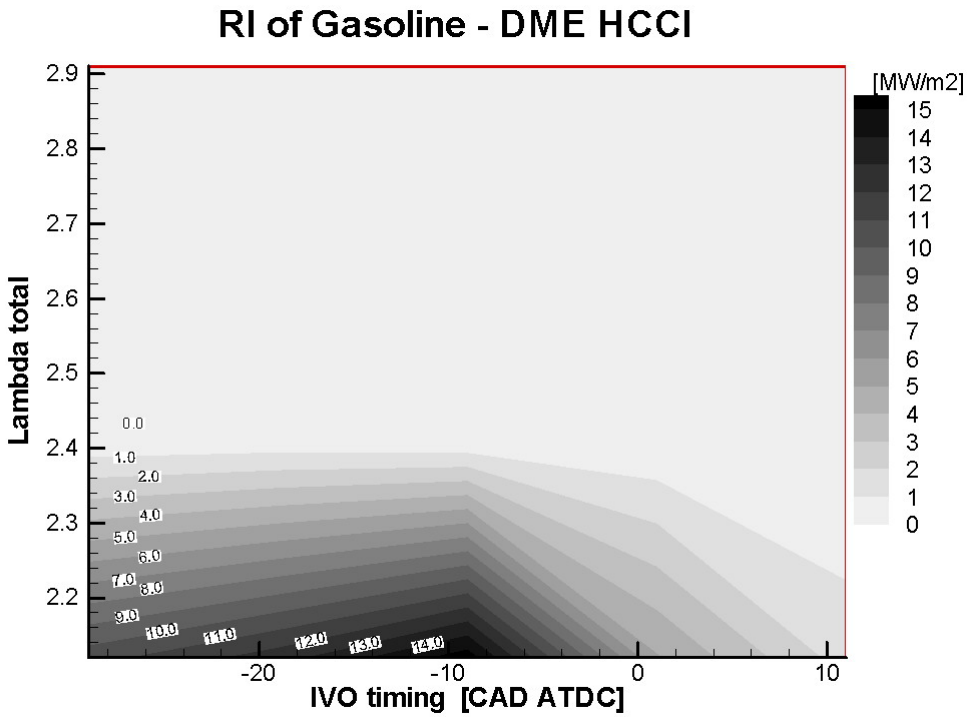

(a) Gasoline-DME HCCI

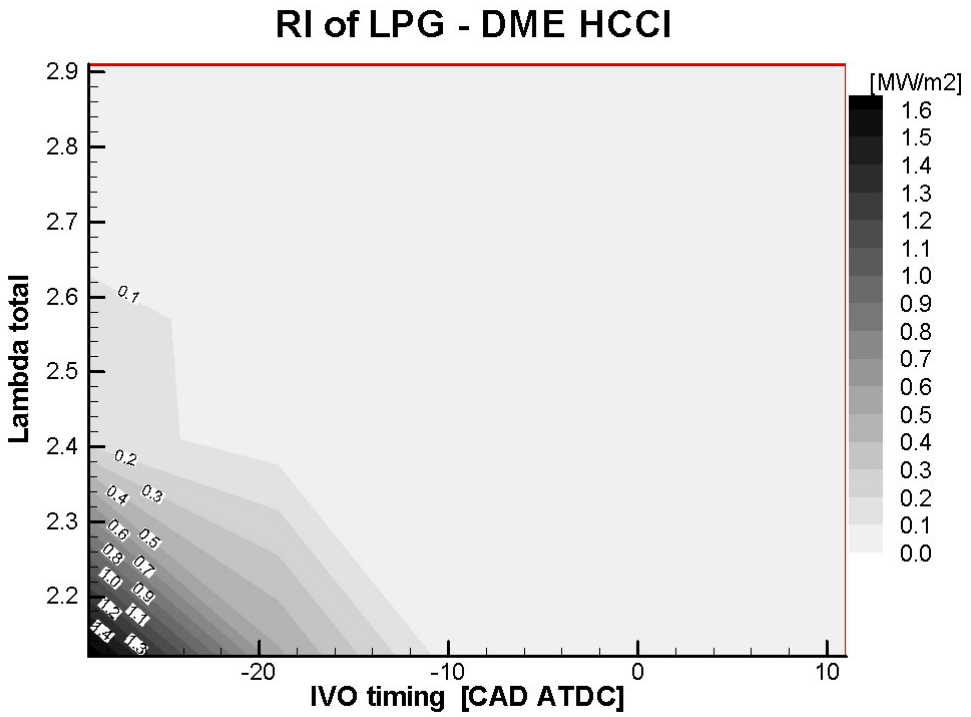

(b) LPG-DME HCCI

Figure 3 RI of HCCI combustion with respect to λ_{TOTAL} and IVO timing at 1000 rpm. (a) Gasoline-DME HCCI (b) LPG-DME HCCI

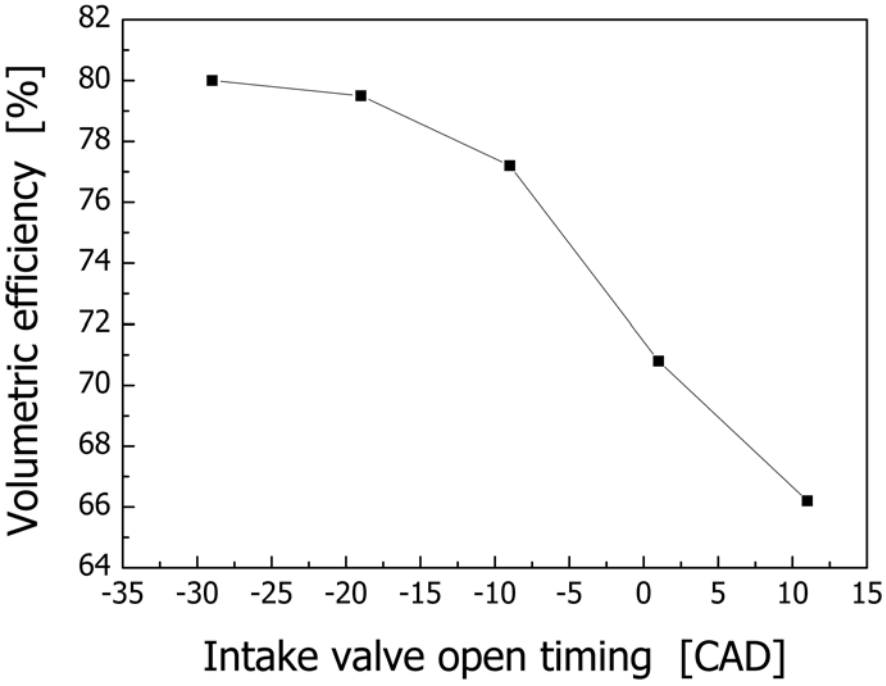

Figure 4 η_v of HCCI combustion with respect to IVO timing.

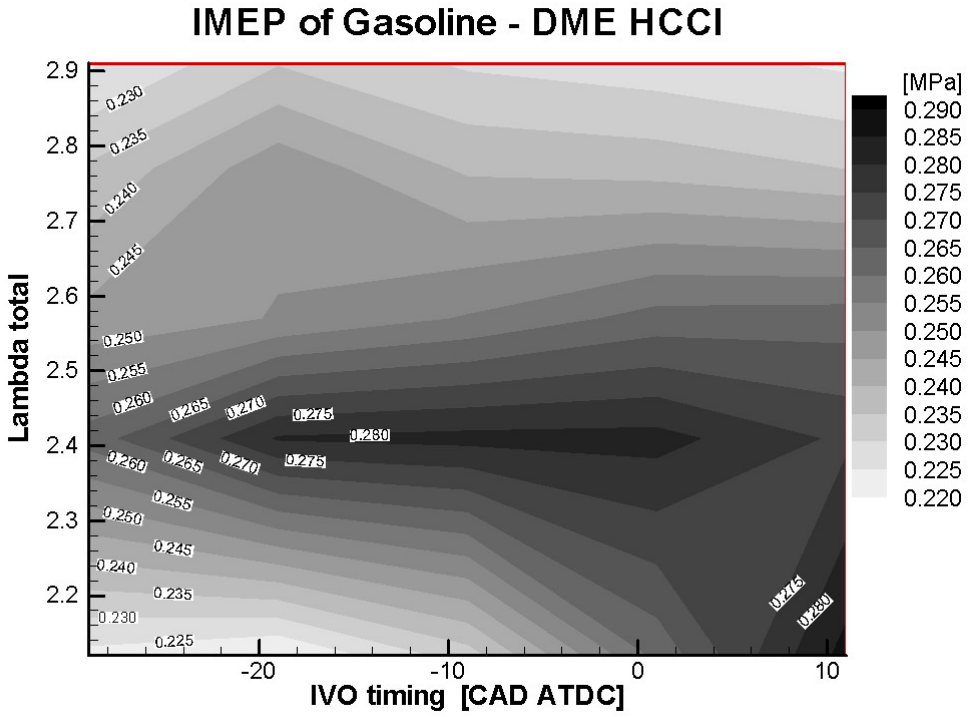

(a) Gasoline-DME HCCI

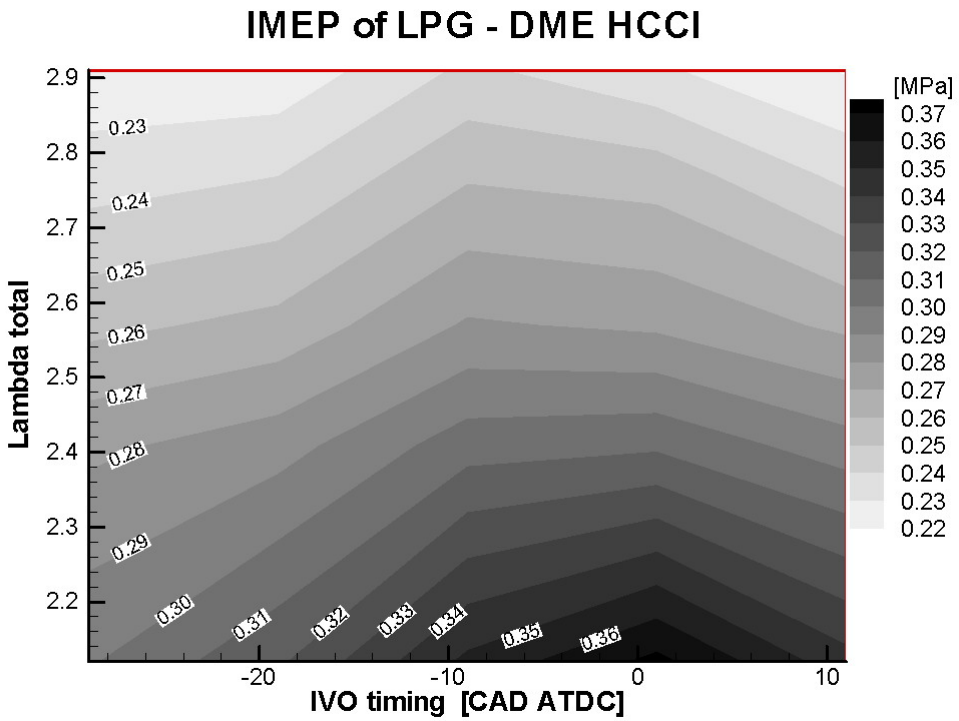

(b) LPG-DME HCCI

Figure 5 IMEP of HCCI combustion with respect to λ_{TOTAL} and IVO timing at 1000 rpm. (a) Gasoline-DME HCCI (b) LPG-DME HCCI

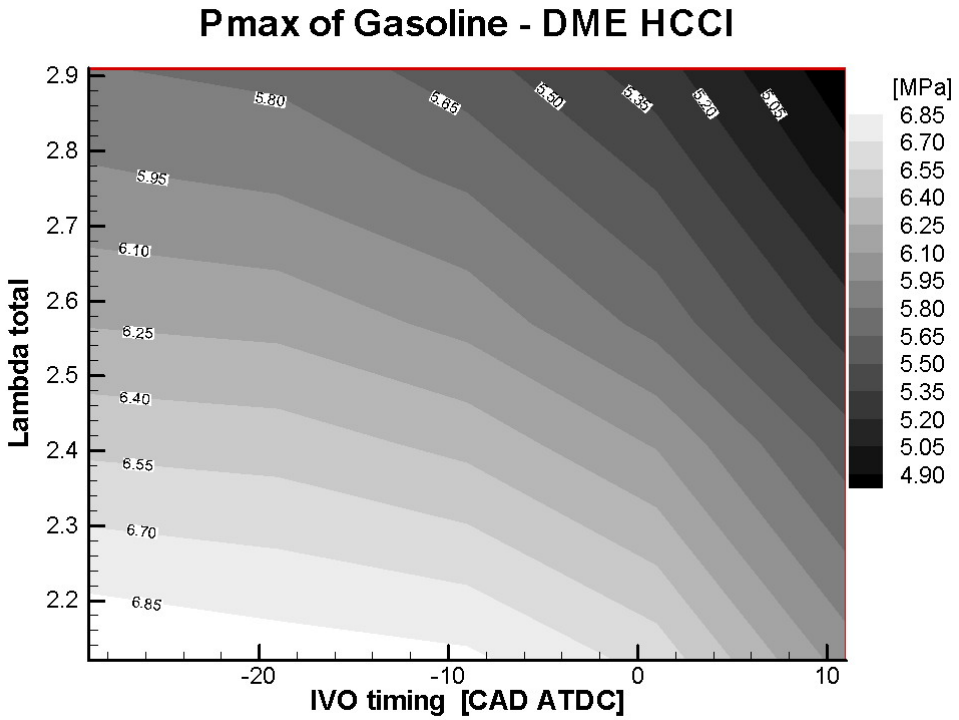

(a) Gasoline-DME HCCI

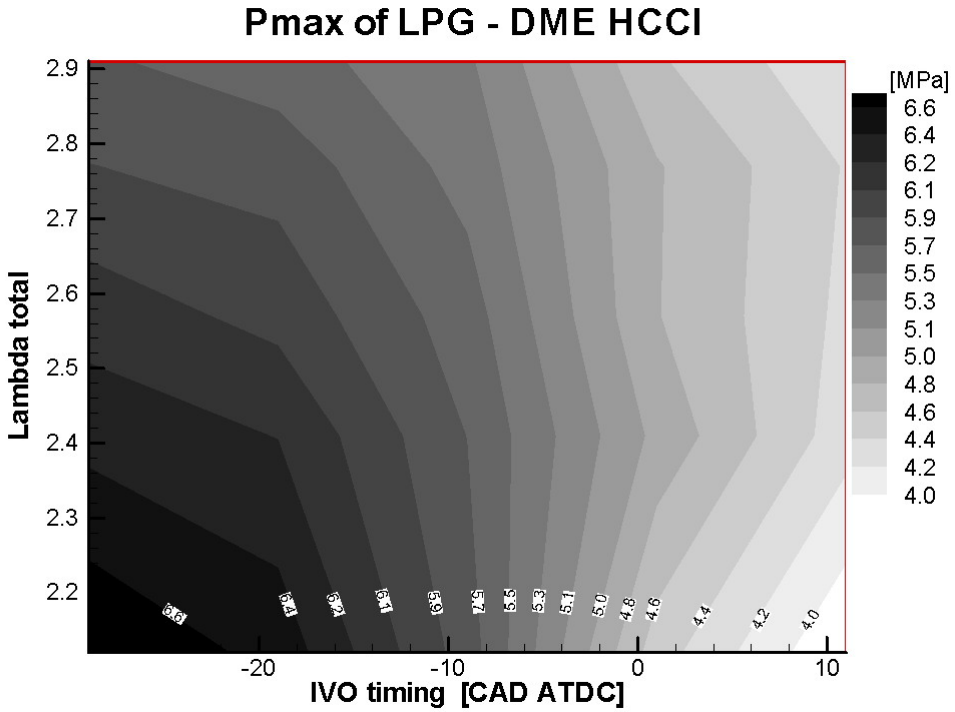

(b) LPG-DME HCCI

Figure 6 P_{max} of HCCI combustion with respect to λ_{TOTAL} and IVO timing at 1000 rpm. (a) Gasoline-DME HCCI (b) LPG-DME HCCI

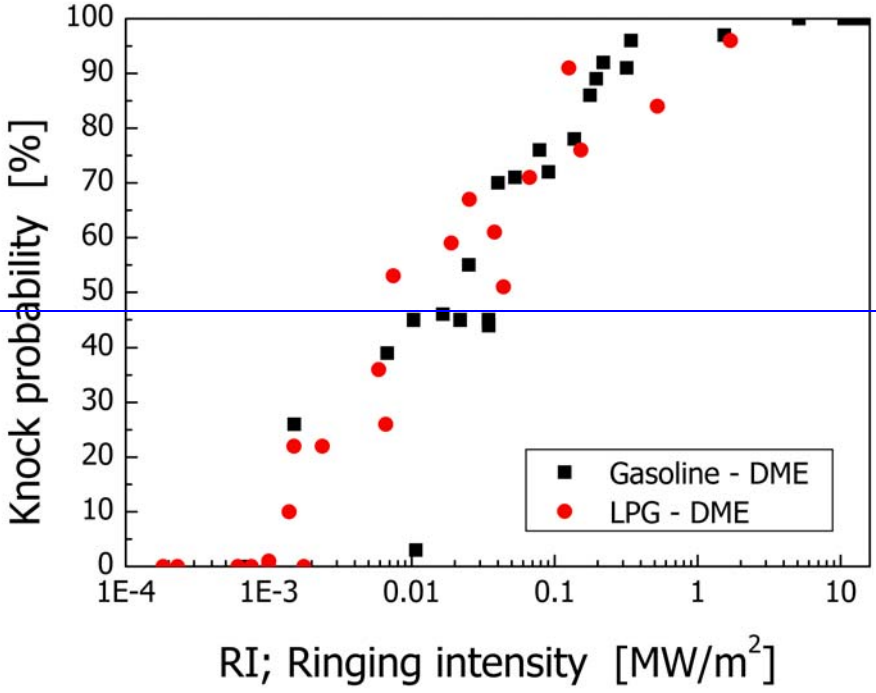

~~Figure 7 Knock probability of HCCI combustion with respect to RI at 1000 rpm.~~

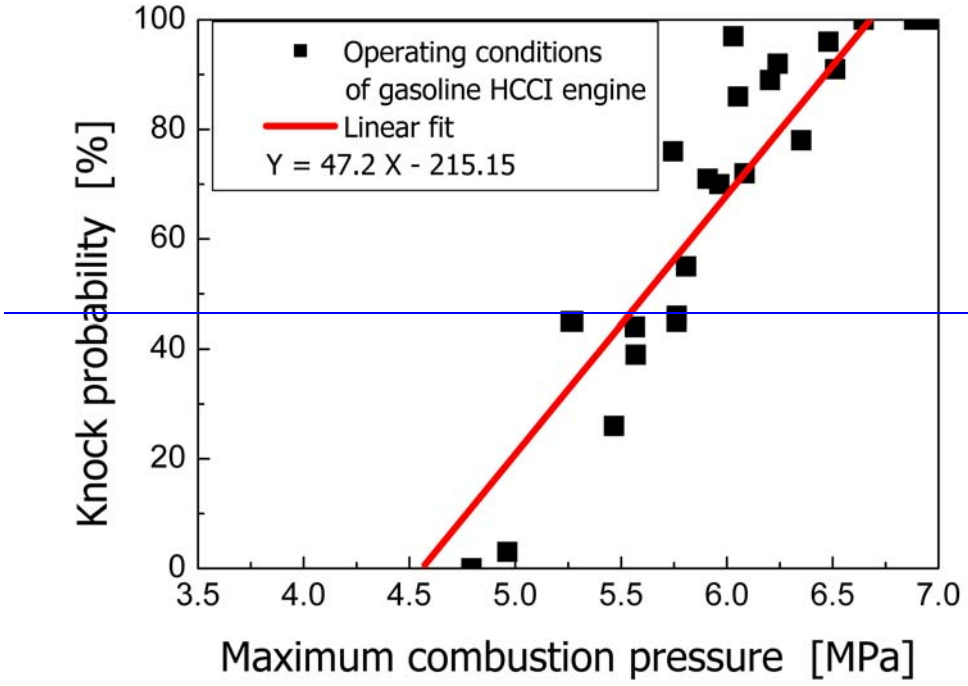

(a) Gasoline-DME HCCI

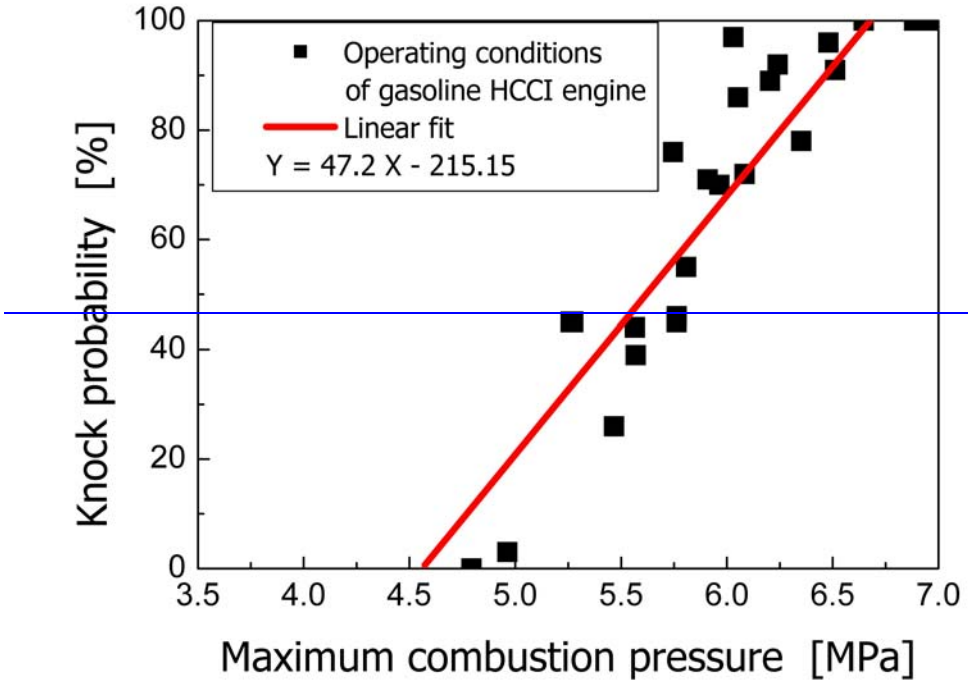

(b) LPG-DME HCCI

Figure 8 Knock probability of HCCI combustion with respect to P_{max} at 1000 rpm. (a) Gasoline-DME HCCI (b) LPG-DME HCCI

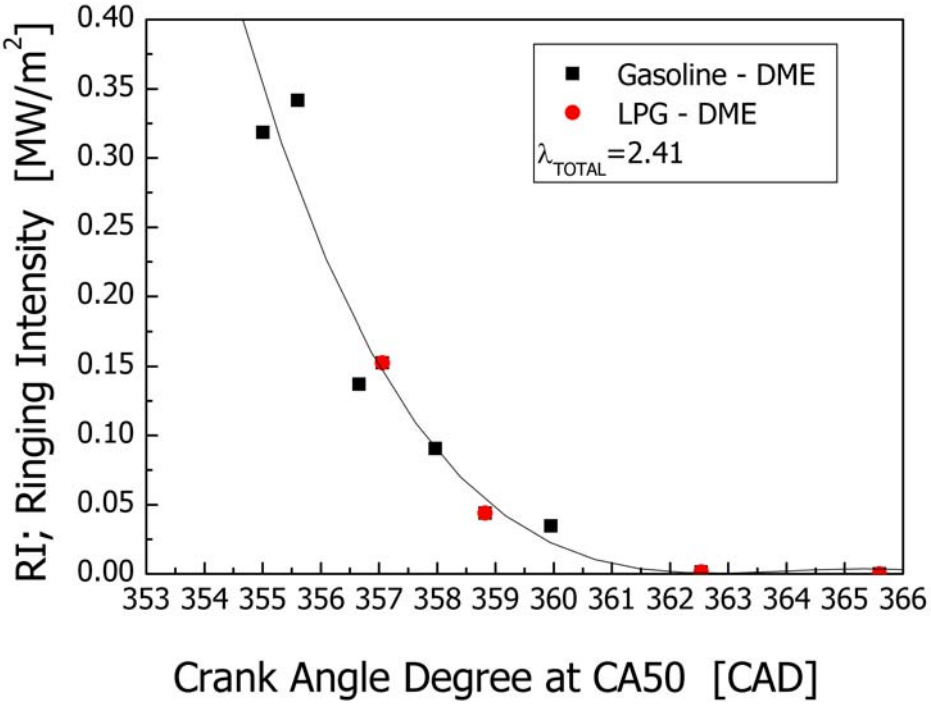

(a) λ_{TOTAL} = 2.41

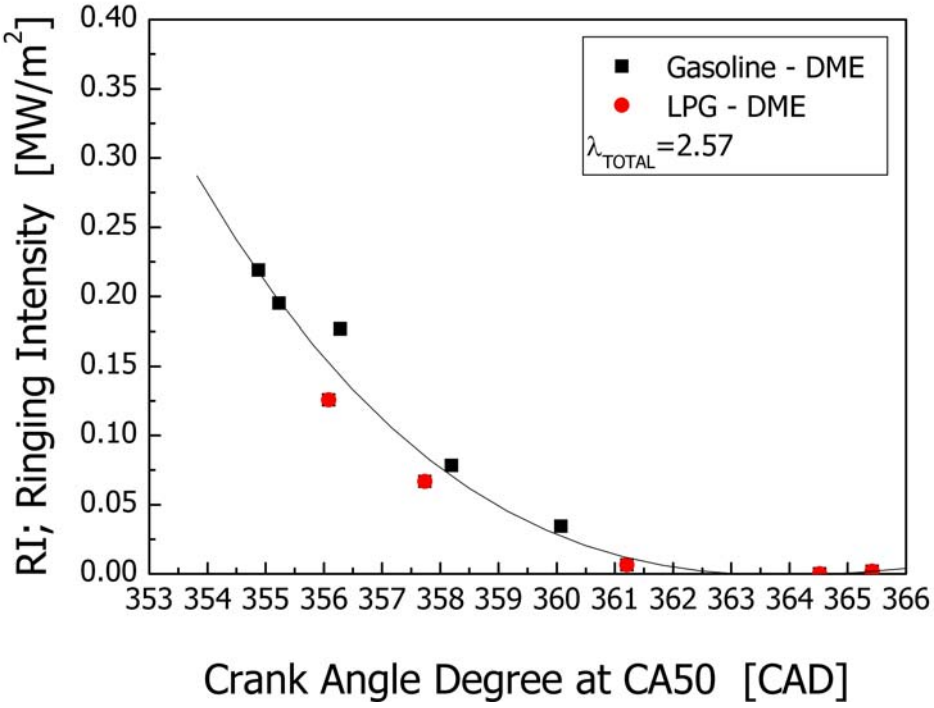

(b) λ_{TOTAL} = 2.57

Figure 9 RI of HCCI combustion with respect to CAD at CA50 and 1000 rpm. (a) $\lambda_{TOTAL} = 2.41$ (b) $\lambda_{TOTAL} = 2.57$

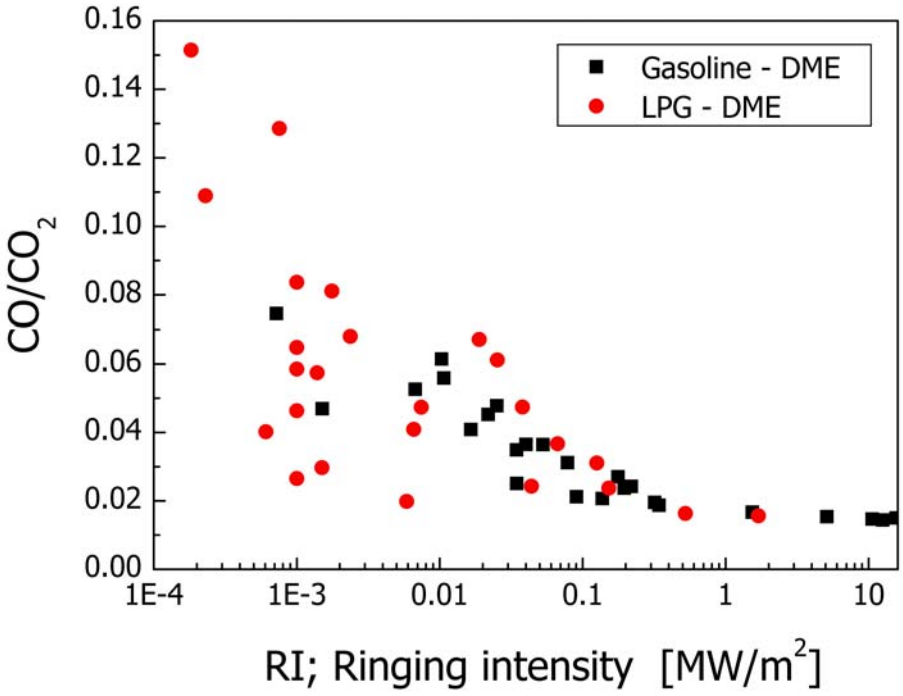

(a) CO / CO_2 emission ratio

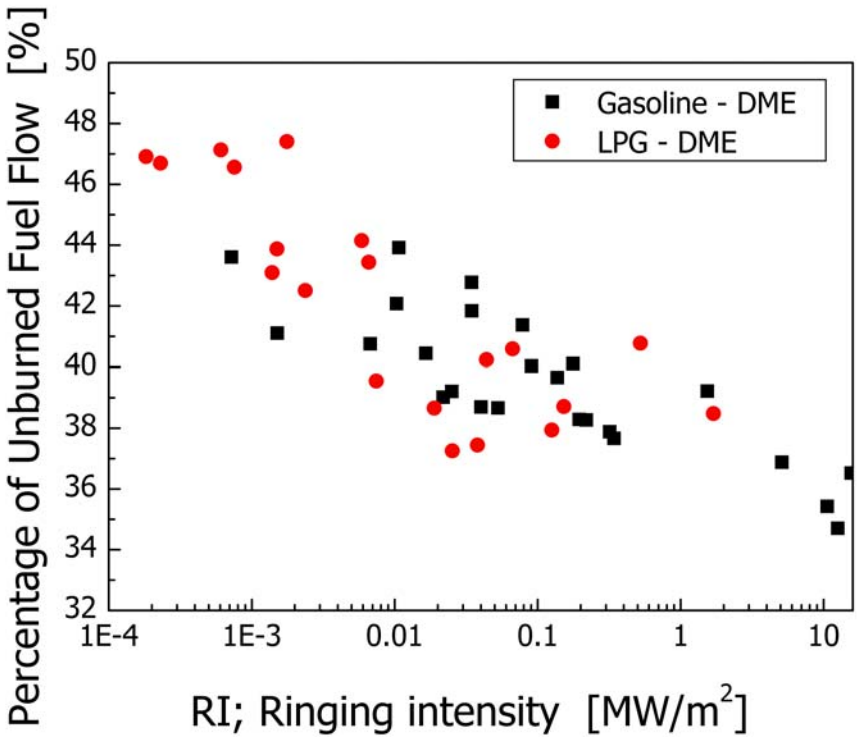

(b) HC emission (as percentages of the total carbon in the initial fuel charge)

Figure 10 Exhaust emissions of HCCI combustion with respect to RI at 1000 rpm. (a) CO / CO_2 emission ratio (b) HC emission (as percentages of the total carbon in the initial fuel charge)

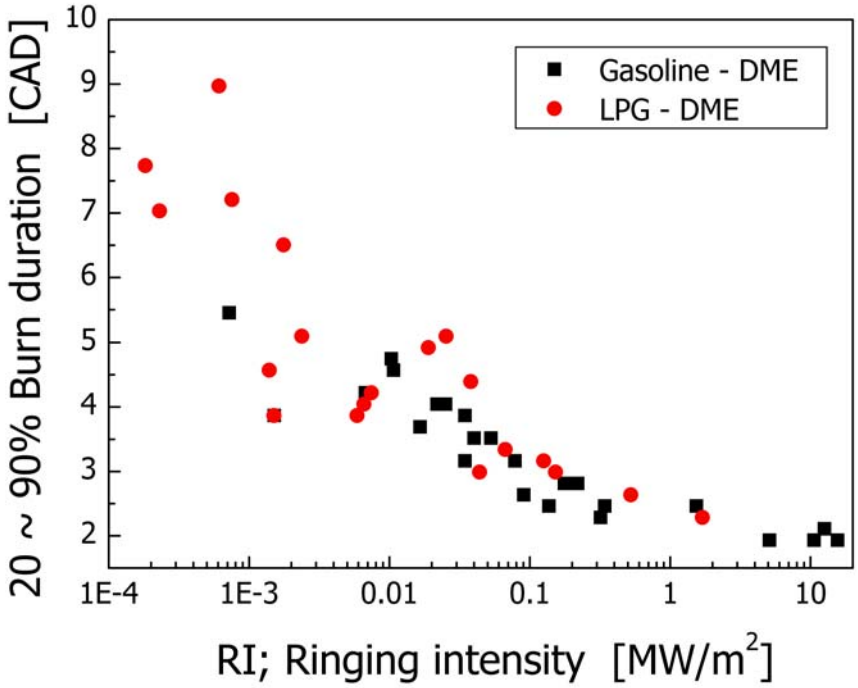

Figure 11 Burn duration of HCCI combustion with respect to RI at 1000 rpm.

List of Tables

Table 1
Engine specifications

Bore (mm)		82
Stroke (mm)		93.5
Compression ratio		13
Displacement (cc)		494
Intake / Exhaust valve opening duration (CAD)		228 / 228
Intake / Exhaust valve lift (mm)		8.5 / 8.4
Valve timing (CAD)	Intake Valve Open (ATDC)	-29 to 11
	Intake Valve Close (ABDC)	59 to 19
	Exhaust Valve Open (BBDC)	42
	Exhaust Valve Close (ATDC)	6
DME injection pressure (MPa)		5
LPG injection pressure (MPa)		1.5
Gasoline injection pressure (MPa)		0.3
DME injector		Slit injector
LPG injector		Single hole port fuel injector
Gasoline injector		Multi hole port fuel injector

Table 2
Experimental conditions

Engine speed (rpm)	1000
Intake Valve Open timing (CAD)	-29, -19, -9, 1, 11
DME injection timing (CAD)	110
LPG and gasoline injection timing (CAD)	470
λ_{TOTAL}	2.12, 2.41, 2.57, 2.77, 2.91
λ_{DME}	3.70
λ_{LPG} and $\lambda_{gasoline}$	4.96, 6.91, 8.42, 11.02, 13.63
Intake charge temperature (^{o}C)	30
Coolant / Oil temperature (^{o}C)	80 / 80